Research article

Lipu Liu, Dong Yang, Weiping Wan, Hong Yang, Qihuang Gong and Yan Li*

Fast fabrication of silver helical metamaterial with single-exposure femtosecond laser photoreduction

https://doi.org/10.1515/nanoph-2019-0079
Received March 10, 2019; revised April 24, 2019; accepted April 26, 2019

Abstract: Metallic helical metamaterials have become the prominent candidates for circular polarizers and other optical-chiral devices as they exhibit strong circular dichroism at a broad operation bandwidth. However, the rapid fabrication of an intertwined double helix with multiple pitch numbers and excellent mechanical strength, electrical conductivity and surface smoothness remains a challenge. We propose and realize the single-exposure femtosecond laser photoreduction of a freestanding, three-dimensional silver double-helix microstructure by the double-helix focal field intensity engineered with a spatial light modulator. At the same time, the photoreduction solution and the laser repetition rate are optimized to further tackle the surface roughness and the thermal flow problems. As a result, the silver double-helix array with the enhanced quality exhibits pronounced optical chirality in a wide wavelength range from 3.5 to 8.5 μm. This technique paves a novel way to easily and rapidly fabricate metallic metamaterials for chiro-optical devices in the mid-infrared regime.

Keywords: metallic helical metamaterial; optical chirality; single-exposure; femtosecond laser photoreduction.

***Corresponding author: Yan Li,** State Key Laboratory for Mesoscopic Physics, Department of Physics, Peking University and Collaborative Innovation Center of Quantum Matter, Beijing 100871, China; and Collaborative Innovation Center of Extreme Optics, Shanxi University, Tianyuan, Shanxi 030006, China, e-mail: li@pku.edu.cn. https://orcid.org/0000-0003-0607-3166
Lipu Liu, Dong Yang and Weiping Wan: State Key Laboratory for Mesoscopic Physics, Department of Physics, Peking University and Collaborative Innovation Center of Quantum Matter, Beijing 100871, China
Hong Yang and Qihuang Gong: State Key Laboratory for Mesoscopic Physics, Department of Physics, Peking University and Collaborative Innovation Center of Quantum Matter, Beijing 100871, China; and Collaborative Innovation Center of Extreme Optics, Shanxi University, Tianyuan, Shanxi 030006, China

1 Introduction

Metallic helical metamaterials, which consist of subwavelength metallic helix unit cells, can exhibit strong circular dichroism at a broad operation bandwidth, thus making them prominent candidates for circular polarizers and other chiral devices [1–4]. To ensure a broad bandwidth or a high extinction ratio, high-quality intertwined helixes with multiple pitch numbers are desired, making the direct fabrication a big challenge [5, 6]. Nonetheless, three prominent approaches have emerged over the past decade: focused-ion-beam induced deposition (FIBID) [1–4, 7–8], glancing angle deposition (GLAD) [1–4, 9–12] and direct laser writing (DLW).

DLW using two-photon polymerization (TPP) can write arbitrary, three-dimensional (3D) nano/microstructures to create a polymer template [1–4, 13–16]. To realize a metallic helical metamaterial, sequential processes, including metal deposition, are required [1–4, 17–19]. At the same time, the multi-photon-induced photoreduction of metal ions in an aqueous solution has been developed for direct writing of a 3D metal microstructure [20–24]. The microstructure in this single-step multiphoton photoreduction (MPR) is assembled point-by-point and formed by the nucleation of small metallic nanoparticles (NPs). During the scanning of the focal spot, the inevitable over exposing or extra thermal flow to the photoreduced NPs in the vicinity deteriorates the uniformity of the size, shape and spacing of these NPs [25]. The final 3D microstructures usually exhibit weak mechanical strength or poor electrical conductivity or rough surface smoothness when the height is greater than a few microns, resulting in the lack of optical function.

In this paper, we propose and realize a single-exposure femtosecond laser photoreduction of a 3D silver microstructure by the focal field engineering using a spatial light modulator (SLM) to shape the incident wavefront [26–30]. The focal field intensity distribution is shaped from an ellipsoid for the conventional Gaussian beam into the double helix in order to simultaneously

photoreduce a freestanding 3D silver double-helix microstructure without scanning. At the same time, the photoreduction solution with both the reductant as well as the growth inhibitor and the laser repetition rate are optimized to further tackle the surface roughness and the thermal flow problems. As a result, the silver double-helix array with the enhanced quality exhibits pronounced transmission distinction for the left circular polarized (LCP) and the right circular polarized (RCP) light in a wide wavelength range from 3.5 to 8.5 μm. This technique paves a novel way to easily and rapidly fabricate metallic metamaterials for chiro-optical devices in the mid-infrared regime.

2 Results and discussion

In the proposed single-exposure MPR as shown in Figure 1, all the parts of a helical microstructure are exposed and heated simultaneously to improve its quality and performance. Although we have demonstrated the single-exposure femtosecond laser TPP of a double-helix microstructure by the focal field engineering with the SLM, a 3D freestanding metallic helical metamaterial with functionality is still difficult to achieve [26].

In TPP via the link of monomers, the polymerized structures only slightly change their refractive index from the unpolymerized material to enable the sub-diffraction limit spatial resolution at tens of nanometers. On the contrary, in the MPR via the nucleation of small metallic NPs reduced from metal ions in the aqueous solution, the photoreduced metal structures are radically different from the solution, resulting in the rough surface or weak mechanical strength or poor conductivity, as shown in the 3D freestanding metallic microstructures fabricated via direct writing MPR, such as a gate, a cup and pyramid arrays [20, 21, 31]. Therefore, we further optimized the components of the solution and the repetition rate of the femtosecond laser to alleviate the aggregation of the NPs and the overheating of the photoreduced parts.

To take advantage of the reductant and the growth inhibitor [21, 32], we developed a photoreduction solution that simultaneously contained the reductant (trisodium citrate) and the growth inhibitor (NDSS: n-decanoylsarcosine sodium), in addition to the silver source ($AgNO_3$) and ammonia in Milli-Q water. A similar solution has just

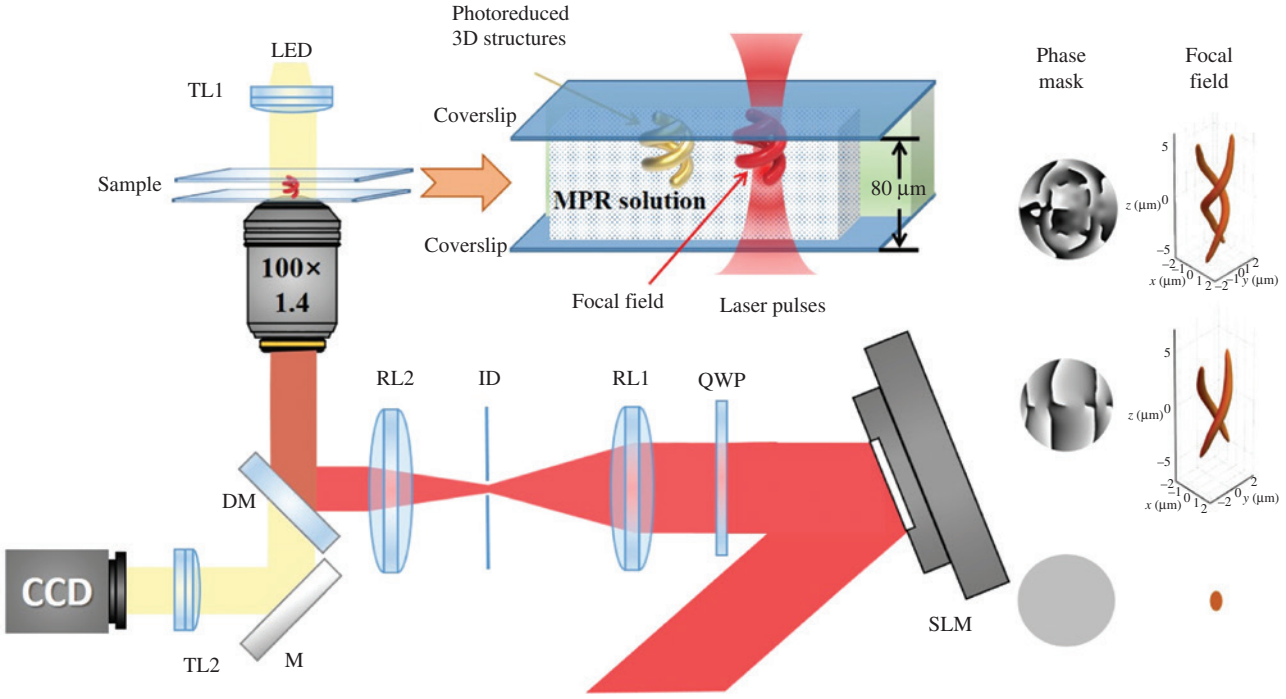

Figure 1: The schematic of the experimental setup for the single-exposure MPR.
A double-helix focal field is generated by the wavefront shaping using a phase-only hologram loaded on a spatial light modulator (SLM). In the conventional direct writing approach, the phase is uniform, resulting in a simple ellipsoidal focus. QWP, quarter wave plate; RL1 and RL2, relay lenses; ID, iris diaphragm; DM, dichroic-mirror; LED, light emitting diode; TL1 and TL2, tube lens; M, mirror; CCD, charge-coupled device.

been used to photoreduce stable 2.5-dimensional shell structures [33].

To verify the improvement of the solution, we photoreduced silver nanowires by direct laser writing at scanning speed of 5 μm/s with laser power of 0.2 mW. When only the reductant was added to the $AgNO_3$ solution, a photoreduced silver nanowire had a line width of ~399 nm with rougher surface and edges (Figure 2A). When only the growth inhibitor was added to the $AgNO_3$ solution, an improved resolution of 220 nm as obtained (Figure 2B). The smallest linewidth of ~200 nm with a smoother surface was obtained using solutions containing both the reductant and the growth inhibitor (Figure 2C and D).

Moreover, the repetition rate of the femtosecond laser pulse was selected to be 100 kHz to avoid the local overheating, which was generated due to the strong light absorption and scattering of reduced silver NPs. When the repetition rate was 80 MHz, the local heating could boil the solution and create bubbles to destroy the fabricated structures. [31] The obvious local heat still appeared even when the repetition rate was 1 MHz in our experiments. Therefore, a repetition rate of 100 kHz was chosen to avoid the heating and still guarantee a relatively fast fabrication speed as much as possible.

A double-helix focal field in Figure 3A was generated by the wavefront shaping using a phase-only hologram on a SLM. The hologram was obtained by optimizing the wavefront of the double-helix beam generated by the equally weighted linear superposition of Laguerre-Gauss (LG) modes with indices (1,1), (3,5), (5,9), (7,13), (9,17) lying along a straight line with a slope of 2 in the LG modal plane [26, 27]. Further details regarding the generation of the double-helix beam and the calculation of its focal intensity can be found in the Supplementary Material. Figure 3B shows a silver double-helix array with period of 3.5 μm. The actual pitch number is ~0.25. Each silver double-helix was fabricated by single exposure for 1.5 s at the exposure power of 120 mW using the 240 fs laser pulses at 1030 nm and 100 kHz. It would take least 30 s to fabricate using DLW [20]. With the single-exposure MPR, the whole process is shortened about 20 times, paving the way for the fast fabrication of silver double-helix metamaterials. The surface roughness is ~200 nm and the conduction is $\sim 3\times10^5$ S/m. These values are close to those of the 2.5-dimensional silver microstructures reported in Ref. [33], which can be improved by thermally annealed in a nitrogen environment.

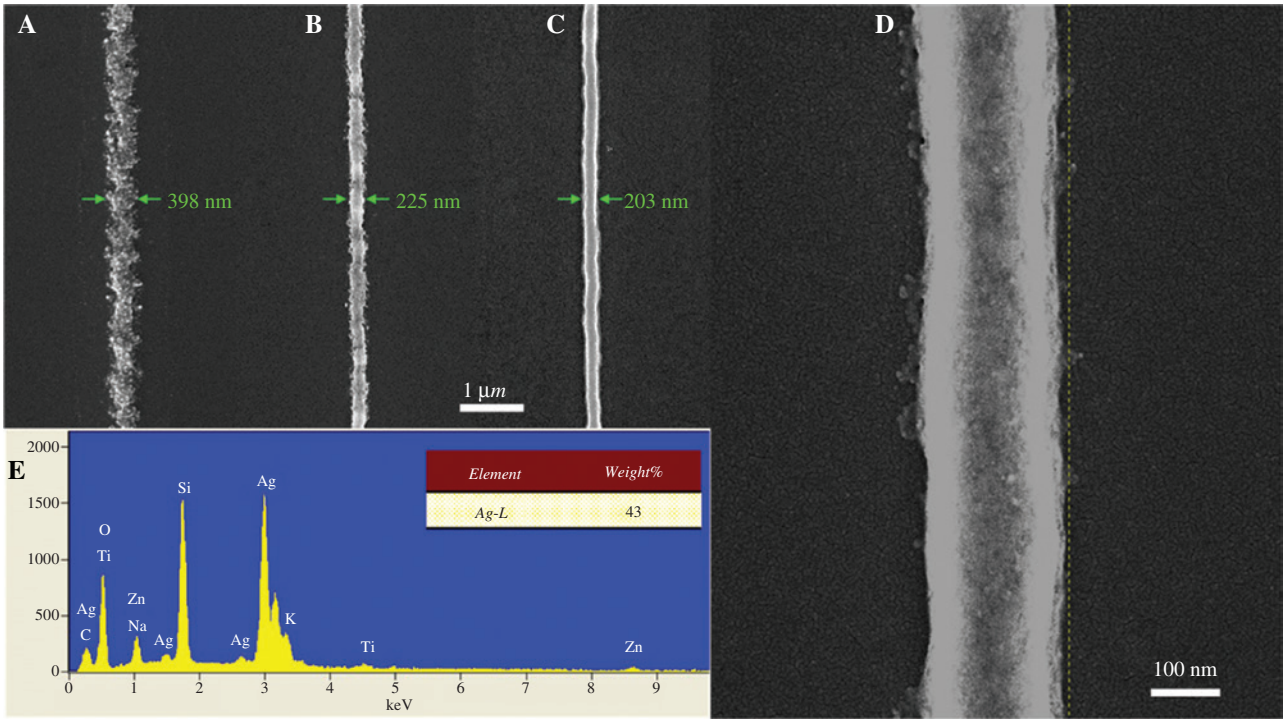

Figure 2: The SEM images of silver nanowires fabricated using the photoreduction solution containing the reductant or growth inhibitator. (A) Reductant only, (B) Growth inhibitor only, (C) Both the reductant and growth inhibitator. (D) The silver nanowires using photoreduction solution composed of $AgNO_3$, trisodium citrate and NDSS. (E) The energy-dispersive X-ray spectroscopy of the reduced silver structures on coverslip.

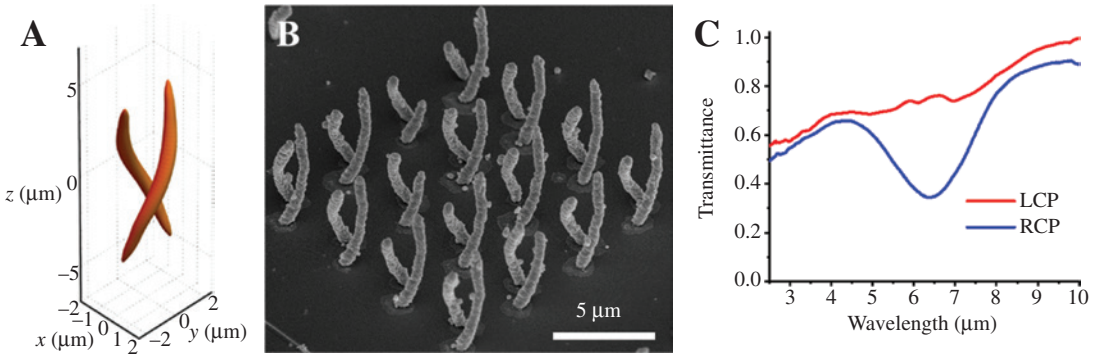

Figure 3: The photoreduction of silver double helix with double-helix beam superposed with LG modes: (1,1), (3,5), (5,9), (7,13), (9,17). (A) The double-helix focal intensity distribution. (B) The SEM images of an array of silver double helix. (C) The measured transmittances of the double-helix silver array for LCP and RCP light at normal incidence.

The chirality of the silver double-helix array was characterized by Fourier transform infrared (FTIR) microscope spectrometer. Figure 3C shows the measured transmittance for normally incident LCP and RCP light. An obvious transmittance difference occurs in the wavelength range from 5.5 to 7.5 μm and a maximum of 41% at a wavelength 6.4 μm. To the best of our knowledge, this is the first realization of 3D functional metallic helical metamaterial using MPR. The discrepancy between the experimental measurement in Figure 3C and the simulated result in Figure S6A in the Supplementary Material may be due to the surface roughness and the impurity of the reduced double helix.

To achieve a broader bandwidth or a higher extinction ratio of the double-helix metamaterials, a double helix with more pitch numbers is required [1–6]. For the single-exposure MPR, one way is to increase the slope of the straight line chosen in LG modal plane as the pitch number is proportional to the slope [34, 35]. When the double-helix focal field is formed by the equally weighted superposition of LG modes with indices (1,1), (3,7), (5,13), (7,19), (9,25) lying along a straight line with slope of 3 in the LG modal plane, the pitch number increases from 0.5 to 1.1.

Unfortunately, this intensity distribution cannot be directly used in TPP or MPR even if the amplitude and the phase are both encoded. There are relatively strong side lobes that cause the severe adhesion of the two main lobes during TPP. To solve this serious problem, we propose an optimization procedure based on the vector diffraction theory, due to the high numerical lens used in the fabrication; we aim to minimize the side lobes by applying constraints in the spatial domain and Fourier domain using double Gaussian and step functions [27]. Further details regarding the optimization procedure can be found in the Supplementary Material. The optimized phase-only hologram can efficiently reconstruct an intertwined double helix with two separated main lobes and greatly suppressed side lobes while maintaining the high pitch numbers, as shown in Figure 4A. It is verified by the TPP of a high-quality double helix in Figure 4B using the resist SZ2080 from FORTH, Greece.

With the optimized double helix in the focal field, a silver double helix with pitch number of ~0.75 in Figure 4C and D with surface roughness of ~180 nm is photoreduced by a single exposure within 1 s at a lower exposure power of 50 mW. According to the smoothness shown in Figures 2D and 4D, the surface roughness of the silver double helix might be caused by the scattering and extra thermal flow of the photoreduced silver structure during the exposure, which may be improved by using lower laser power or repetition rate at a cost of longer exposure time.

The fabricated silver double-helix array in Figure 4E exhibits enhanced transmission difference for LCP and RCP light in a wide wavelength range from 3.5 to 8.5 μm, which exceeds one octave, as demonstrated in Figure 4F. Again, the discrepancy between Figures 4F and S6C may be due to the surface roughness and the impurity of the reduced double helix. The extinction ratio might be further improved using a double helix with more pitch numbers.

3 Conclusion

In conclusion, using the single-exposure femtosecond laser photoreduction benefiting from the focal field engineering, we have demonstrated the rapid fabrication of a freestanding, silver double-helix array exhibiting pronounced optical chirality in a wide wavelength range

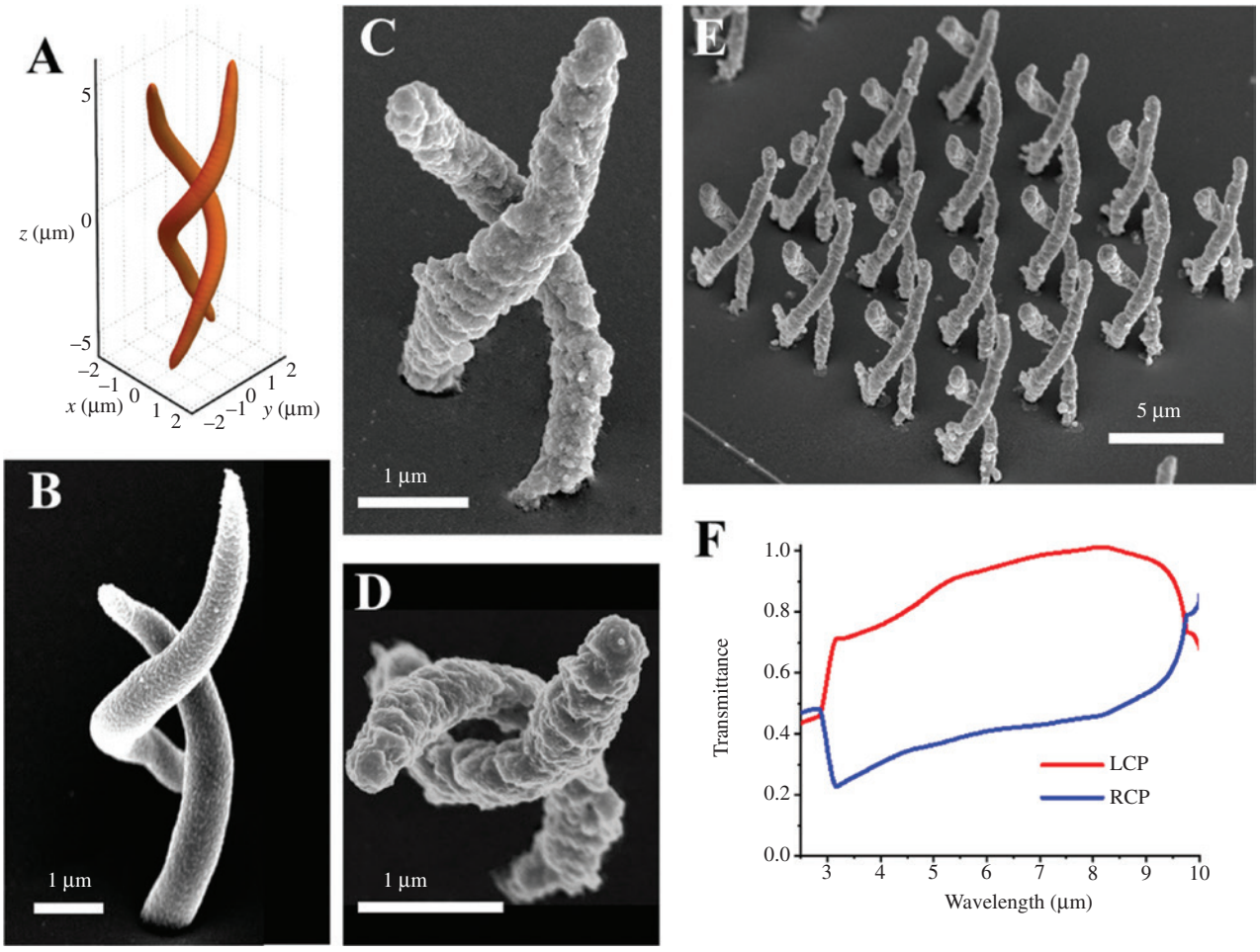

Figure 4: The photoreduction using the optimized double-helix focal field.
(A) The optimized double-helix focal intensity distribution from the superposition of the LG modes with indices (1,1), (3,7), (5,13), (7,19) and (9,25). (B) The SEM images of a single, two-photon polymerized double helix. (C, D) The SEM images of a single photoreduced silver double helix. (E) The SEM image of a silver double-helix array. (F) The measured transmittance spectra of the silver double-helix array for LCP and RCP light at normal incidence.

from 3.5 to 8.5 μm. This technique provides a key option to enable the easy and rapid fabrication of metallic metamaterials for chiro-optical devices in the mid-infrared regime.

4 Methods

4.1 Experimental setup

The experimental setup is adapted from the direct laser writing system by inserting a spatial phase modulator to shape the wavefront of the incident beam, as demonstrated in Figure 1. A mode-locked regenerative amplified Yb:KGW-based femtosecond laser system (PHAROS, Light Conversion), operates at a wavelength of 1030 nm with a pulse duration of ~230 fs and repetition rates up to 1 MHz is utilized as an excitation source. A variable attenuator consisting of a half wave plate and a polarizer can adjust the power that delivered to the sample. The expanded laser beam impinges on a reflective phase-only SLM (X10468-03, Hamamatsu), transforming the Gaussian beam into an engineered beam. The linearly polarized light is turned into a circularly polarized beam by a quarter wave plate (QWP). The resulting beam is then relayed using a Keplerian telescope consisting of the relay lenses RL1 (focal length of 1000 mm) and RL2 (focal length of 750 mm), thus allowing it to fully illuminate the back aperture of the microscope objective lens (1.4 NA, 100×, Olympus). Finally, the engineered beam is focused into the sample to initiate the photoreduction. Instead of the commonly

used one coverslip configuration, the photoreduction solution is sandwiched between two coverslips using a polyimide tape as a spacer. The laser beam passes through the bottom coverslip (borosilicate glass), after which it is focused at the bottom surface of the top coverslip (CaF_2) and the silver double helix structure is fabricated on the bottom surface of the top coverslip. The sample is then mounted on a high precision XYZ linear air-bearing translation stage (Areotech) controlled by computer. A LED illuminates the sample, which is imaged on the CCD camera using the tube lens (TL2, focal length of 200 mm) in combination with a dichroic-mirror filter (DM) that prevents the backscattered laser light from saturating the camera.

4.2 Sample preparation

The photoreduction solution contains three components, including a reducing agent, a growth inhibitor and a source of silver. Trisodium citrate is used as the reducing agent, N-decanoylsarcosine sodium (NDSS) is used as the growth inhibitor, and silver nitrate ($AgNO_3$) is used as the source of silver. Trisodium citrate (99%), $AgNO_3$ (99 + %) and ammonia (25%wt) are purchased from Alfa Aesar (China) Chemicals Co., Ltd. NDSS (98 + %) is purchased from Tokyo Chemical Industry Co., Ltd. The solution is prepared by mixing the trisodium citrate, NDSS, silver nitrate, ammonia in Milli-Q water with the concentrations of 0.05, 0.01, 0.2 and 0.4 M, respectively.

4.3 Sample characterization

After fabrication, the sample is rinsed by double-distilled water and dried in critical point dryer. The morphology and component of silver microstructures are characterized by scanning electronic microscope (FEI Helios Nanolab 600i). A commercial FTIR microscope spectrometer (Bruker 70 with Bruker Hyperion 1000) is used to characterize the optical functionalities of the fabricated structures.

To verify whether the fabricated structure is silver, energy-dispersive X-ray spectroscopy (EDS) is performed during the scanning electron microscopic (SEM) measurement of the fabricated structures. The Ag specie with weight of ~43% can be clearly seen from the data in Figure 2E, while the other species are from the cover glass substrate.

Acknowledgments: This work was supported by research grants from the National Key R&D Program of China under Grant Nos. 2018YFB1107205 and 2016YFA0301302 and by the National Natural Science Foundation of China under Grant Nos. 61590933, 11474010 and 11627803.

References

[1] Gansel JK, Thiel M, Rill MS, et al. Gold helix photonic metamaterial as broadband circular polarizer. Science 2009;325:1513–5.
[2] Kaschke J, Wegener M. Optical and infrared helical metamaterials. Nanophotonics 2016;5:510–23.
[3] Li Q, Grojo D, Alloncle A-P, Chichkov B, Delaporte P. Digital laser micro- and nanoprinting. Nanophotonics 2018;8:27–44.
[4] Qiu M, Zhang L, Tang Z, Jin W, Qiu C-W, Lei DY. 3D Metaphotonic nanostructures with intrinsic chirality. Adv Funct Mater 2018;28:1803147.
[5] Passaseo A, Esposito M, Cuscunà M, Tasco V. Materials and 3D designs of helix nanostructures for chirality at optical frequencies. Adv Opt Mater 2017;5:1601079.
[6] Kaschke J, Gansel JK, Wegener M. On metamaterial circular polarizers based on metal N-helices. Opt Express 2012;20:26012–20.
[7] Esposito M, Tasco V, Cuscuna M, et al. Nanoscale 3D chiral plasmonic helices with circular dichroism at visible frequencies. ACS Photonics 2014;2:105–14.
[8] Esposito M, Tasco V, Todisco F, et al. Triple-helical nanowires by tomographic rotatory growth for chiral photonics. Nat Commun 2015;6:6484.
[9] Mark AG, Gibbs JG, Lee T-C, Fischer P. Hybrid nanocolloids with programmed three-dimensional shape and material composition. Nat Mater 2013;12:802–7.
[10] Singh JH, Nair G, Ghosh A, Ghosh A. Wafer scale fabrication of porous three-dimensional plasmonic metamaterials for the visible region: chiral and beyond. Nanoscale 2013;5:7224–8.
[11] Gibbs JG, Mark AG, Eslami S, Fischer P. Plasmonic nanohelix metamaterials with tailorable giant circular dichroism. Appl Phys Lett 2013;103:213101.
[12] Larsen GK, He YZ, Wang J, Zhao YP. Scalable fabrication of composite Ti/Ag plasmonic helices: controlling morphology and optical activity by tailoring material properties. Adv Opt Mater 2014;2:245–9.
[13] Kawata S, Sun HB, Tanaka T, Takada K. Finer features for functional microdevices. Nature 2001;412:697–8.
[14] Fischer J, Wegener M. Three-dimensional optical laser lithography beyond the diffraction limit. Laser Photon Rev 2013;7:22–44.
[15] Lao Z, Hu Y, Pan D, et al. Self-sealed bionic long microchannels with thin walls and designable nanoholes prepared by line-contact capillary-force assembly. Small 2017;13:1603957.
[16] Hu Y, Miles BT, Ho Y-LD, et al. Toward direct laser writing of actively tuneable 3D photonic crystals. Adv Opt Mater 2017;5:1600458.
[17] Kaschke J, Blume L, Wu L, et al. A helical metamaterial for broadband circular polarization conversion. Adv Opt Mater 2015;3:1411–7.
[18] Kaschke J, Wegener M. Gold triple-helix mid-infrared metamaterial by STED-inspired laser lithography. Opt Lett 2015;40:3986–9.

[19] Gansel JK, Latzel M, Frölich A, Kaschke J, Thiel M, Wegener M. Tapered gold-helix metamaterials as improved circular polarizers. Appl Phys Lett 2012;100:101109.
[20] Ishikawa A, Tanaka T, Kawata S. Improvement in the reduction of silver ions in aqueous solution using two-photon sensitive dye. Appl Phys Lett 2006;89:113102.
[21] Cao YY, Takeyasu N, Tanaka T, Duan XM, Kawata S. 3D metallic nanostructure fabrication by surfactant-assisted multiphoton-induced reduction. Small 2009;5:1144–8.
[22] Xu BB, Xia H, Niu LG, et al. Flexible nanowiring of metal on nonplanar substrates by femtosecond-laser-induced electroless plating. Small 2010;6:1762–6.
[23] Lu WE, Zhang YL, Zheng ML, et al. Femtosecond direct laser writing of gold nanostructures by ionic liquid assisted multiphoton photoreduction. Opt Mater Express 2013;3:1660–73.
[24] Tabrizi S, Cao YY, Cumming BP, Jia BH, Gu M. Functional optical plasmonic resonators fabricated via highly photosensitive direct laser reduction. Adv Opt Mater 2016;4:529–33.
[25] Tabrizi S, Cao YY, Lin H, Jia B. Two-photon reduction: a cost-effective method for fabrication of functional metallic nanostructures. Sci China Phys Mech Astron 2017;60:034201.
[26] Zhang SJ, Li Y, Liu ZP, et al. Two-photon polymerization of a three-dimensional structure using beams with orbital angular momentum. Appl Phys Lett 2014;105:61101.
[27] Li Y, Liu L, Yang D, Zhang Q, Yang H, Gong Q. Femtosecond laser nano/microfabrication via three-dimensional focal field engineering. Laser-based Micro- Nanoprocess XI 2017:100920B.
[28] Zhang Q, Yang D, Qi J, Cheng Y, Gong Q, Li Y. Single-scan femtosecond laser transverse writing of depressed cladding waveguides enabled by three-dimensional focal field engineering. Opt Express 2017;25:13263–70.
[29] Ni JC, Wang CW, Zhang CC, et al. Three-dimensional chiral microstructures fabricated by structured optical vortices in isotropic material. Light Appl 2017;6:e17011.
[30] Shusteff M, Browar AEM, Kelly BE, et al. One-step volumetric additive manufacturing of complex polymer structures. Sci Adv 2017;3:eaao5496.
[31] Tanaka T, Ishikawa A, Kawata S. Two-photon-induced reduction of metal ions for fabricating three-dimensional electrically conductive metallic microstructure. Appl Phys Lett 2006;88:081107.
[32] Jiang XC, Chen CY, Chen WM, Yu AB. Role of citric acid in the formation of silver nanoplates through a synergistic reduction approach. Langmuir 2009;26:4400–8.
[33] Barton P, Mukherjee S, Prabha J, Boudouris BW, Pan L, Xu XF. Fabrication of silver nanostructures using femtosecond laser-induced photoreduction. Nanotechnology 2017;28:505302.
[34] Piestun R, Schechner YY, Shamir J. Propagation-invariant wave fields with finite energy. J Opt Soc Am A 2000;17:294–303.
[35] Pavani SRP, Piestun R. High-efficiency rotating point spread functions. Opt Express 2008;16:3484–9.

Supplementary Material: The online version of this article offers supplementary material (https://doi.org/10.1515/nanoph-2019-0079).